ACS OMEGA

http://pubs.acs.org/journal/acsodf

Article

Hydrotreating of Atmospheric Gas Oil and Co-Processing with Rapeseed Oil Using Sulfur-Free PMoCx/Al_2O_3 Catalysts

Héctor de Paz Carmona,* Eliška Svobodová, Zdeněk Tišler, Uliana Akhmetzyanova, and Kateřina Strejcová

Cite This: *ACS Omega* 2021, 6, 7680−7692

Read Online

ACCESS | Metrics & More | Article Recommendations | Supporting Information

ABSTRACT: Sulfur-free molybdenum carbides have the potential to replace the conventional sulfided catalysts used for hydrotreating. For these catalysts, it is not necessary to add sulfur to maintain their activity. This fact makes it worthwhile to continue working on improving their hydrotreating efficiency. According to our previous studies, the addition of Co or Ni promotes the hydrotreating activity, but only significant in the case of hydrodesulfurization efficiency (up to 30%). To increase the hydrodenitrogenation efficiency, other promoters, such as phosphorus, can be added. However, most of the published studies do not focus on co-processing or only on hydrotreating of gas oil model molecules at a laboratory scale. In this paper, we build on our previous research by studying five sulfur-free phosphorus-modified MoCx/Al_2O_3 catalysts (0.5, 1.5, 2.5, 3.5, and 4.5 wt %) for the hydrotreating of atmospheric gas oil and co-processing with rapeseed oil (5, 10, and 25 wt %) under industrial conditions (330−350 °C, 5.5 MPa, WHSV 1−2 h^{-1}). A phosphorus content up to 1.5 wt % promoted the hydrodesulfurization (5−10%) and the hydrodenitrogenation (10−25%) efficiencies of catalysts. Moreover, the triglycerides addition did not significantly decrease the catalyst activity during co-processing. Therefore, our results enable us to define the range of phosphorus addition that enhances MoCx activity using industrial conditions and commercial feedstocks, pointing the way to develop a suitable and sulfur-free alternative to conventional hydrotreating catalysts.

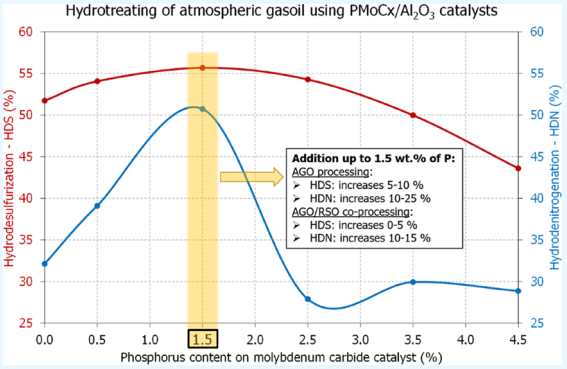

1. INTRODUCTION

The Renewable Energy Directive (RED) of the European Union (EU) establishes an overall target of 32% for renewable energy sources consumption by 2030. This target mandates the development of green and sustainable biofuels capable of replacing conventional petroleum fuels.

The co-processing of petroleum fuels with vegetable oils in hydrotreating units is an interesting and promising route to high-quality biofuel production.[1−4] The co-processing approach has several built-in advantages, including full compatibility with current engines, flexibility in the use of feedstock, and low additional costs, all of which make it suitable for application in existing refineries.[5−7]

Co-processing implies not only the hydrodesulfurization (HDS) and hydrodenitrogenation (HDN) of middle distillates but also the deoxygenation (DO) of triglycerides.[8] DO occurs by a combination of three pathways in the presence of H_2:[9,10] hydrodeoxygenation (HDO), (hydro)decarboxylation, and (hydro)decarbonylation (DCO). These routes all result in linear paraffins with an even (HDO) or odd (DCO) number of carbon atoms (n-C_{15} to n-C_{18}) plus water and light gases (C_3H_8, CO_2, and CO) as side products. The catalyst selected plays an essential role in DO, particularly in pathway selectivity and product distribution.

Conventional hydrotreating catalysts (sulfide CoMo/Al_2O_3 and NiMo/Al_2O_3) work for co-processing.[11−14] However, it is necessary to increase the amount of biomass consumed by co-processing to fulfill the ambitious new EU target. The problem is that an increase in biomass co-processing (i.e., >20 wt %.) significantly reduces the efficiency of conventional catalysts due to the sulfur leaching phenomenon on the catalyst surface.[15,16] Therefore, it is necessary to find and develop new materials that can overcome this problem.

Sulfur-free supported carbide, nitride, or phosphide catalysts (MoCx, MoNx, or MoPx)[17−22] appear to be better candidates for co-processing than conventional ones due to the fact of no sulfur needed to maintain its activity. Moreover, several studies[23−29] have reported significant catalyst activity in the

Received: December 30, 2020
Accepted: March 4, 2021
Published: March 12, 2021

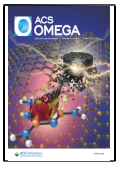

Table 1. Characterization of Fresh PMoCx Catalyst Samples after Passivation

catalyst	MoCx	PMoCx 0.5	PMoCx 1.5	PMoCx 2.5	PMoCx 3.5	PMoCx 4.5
S_{BET} (m^2/g)	143	160	171	141	142	130
metal ICP-OES (%)						
Mo	20.1	17.8	20.6	19.6	18.6	19.6
P	0.0	0.6	1.7	2.7	3.5	5.0
Al	36.7	43.0	41.0	37.2	37.0	36.9
P/Mo (wt %/wt %)	0.00	0.03	0.08	0.14	0.19	0.26
elemental analysis (%)						
C	1.02	0.86	0.96	0.85	1.07	0.99
N	0.05	0.05	0.05	0.05	0.05	0.05

case of triglycerides processing. However, conventional sulfided catalysts seem to be more efficient in hydrotreating yet.[4] Thus, it is mandatory to improve the HDS and HDN efficiencies of sulfur-free catalysts to be considered as a suitable alternative to conventional ones.

As described in previous studies,[30−32] simple means of increasing the activity of sulfur-free catalysts is to add Co or Ni to the catalyst structure. This addition results in a significant increase in HDS, but the HDN is still low. In this sense, phosphorus can be used as an additive to increase catalyst acidity, which promotes active phase surface dispersion, and consequently, the HDN efficiency of MoCx catalysts,[33−35] via a synergistic effect on the active catalyst components.[36,37]

Most of these published studies only involve gas oil model molecules, such as thiophene or dimethyl dibenzothiophene. The knowledge gap is even more significant in co-processing studies, without a relevant number of papers. Here, we fill this knowledge gap by carrying out the detailed research on the hydrotreating of atmospheric gas oil and its blends with rapeseed oil under standard industrial conditions using sulfur-free supported PMoCx catalysts.

In this work, we build on our previous research[24,30] by studying five sulfur-free, Al_2O_3-supported MoCx catalysts containing 0.5, 1.5, 2.5, 3.5, and 4.5 wt % phosphorus for the hydrotreating of atmospheric gas oil (AGO) and co-processing with rapeseed oil (RSO: 5, 10, and 25 wt %) under industrial conditions of 330−350 °C, 5.5 MPa, and a weight hourly space velocity (WHSV) of 1−2 h^{-1}. The PMoCx catalysts' properties are characterized in terms of metal content, Hg porosimetry, H_2 physisorption, elemental analysis, X-ray diffraction (XRD), and temperature-programmed desorption/reduction (TPD/TPR), and catalyst activity is evaluated. The results enable us to define the range of phosphorus addition that significantly improves the MoCx catalyst's activity without a significant loss of activity derived from the vegetable oil addition.

2. RESULTS AND DISCUSSION

2.1. Catalyst Characterization. The phosphorus content was increased from 0.5 to 4.5 wt % in increments of 1 wt %. Table 1 shows the characterization of fresh catalyst samples after passivation. The MoCx catalyst properties were already described in a previous article.[24]

Mo impregnation occurred similarly for all catalyst samples. Elemental analysis shows a mean value of 0.96% C, which indicates that the carburization procedure was successful. The nitrogen content of the samples was small. The increase in the phosphorus content leads to a decrease in specific surface area (S_{BET}). This effect, which was observed in the Hg porosimetry results (Figure 1) as well, together with a decrease in the mean

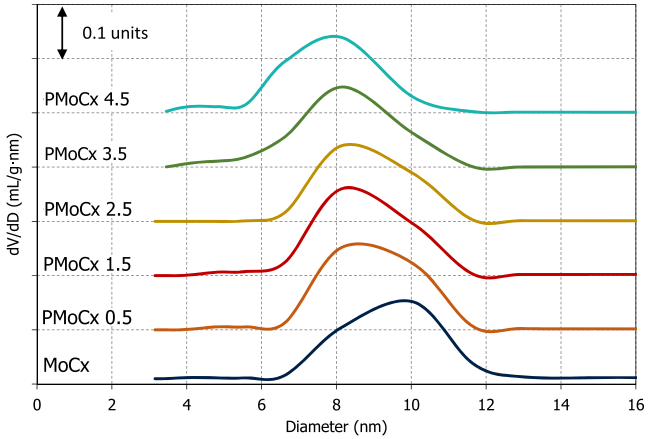

Figure 1. Pore diameter distributions on MoCx and PMoCx catalysts surface measured by Hg-porosimetry.

pore diameter (from 9.5 MoCx to 7.4 nm PMoCx 4.5), might be due to pore-blocking of the catalyst support by P and Mo compounds.[33,34,39] This fact should not affect catalyst activity due to changes produced in other properties, as described later.

XRD analysis is not suitable for describing in detail amorphous Al_2O_3-supported catalysts. However, this technique allows identifying and determining the main phases present in the samples. Figure 2 shows the XRD diffraction patterns of fresh PMoCx catalysts after passivation, with the main phases marked. As expected, the XRD results reveal catalyst samples of low crystallinity with a dominant amorphous phase, wherein the peaks corresponding to the Al_2O_3 support (PDF 46-1215)

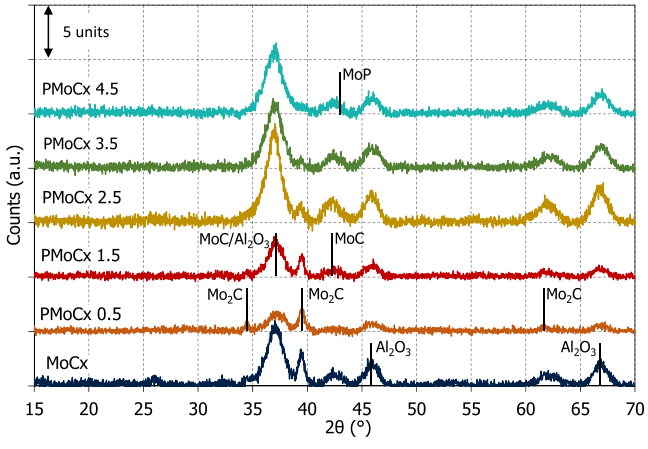

Figure 2. XRD spectra of MoCx and PMoCx catalysts after passivation. Marks indicate the main phases detected.

https://dx.doi.org/10.1021/acsomega.0c06336
ACS Omega 2021, 6, 7680−7692

are easy to detect. The absence of peaks corresponding to MoO_2/tugarinovite (2θ = 26.0, 37.0, and 37.3; PDF 86-0135) and the presence of MoCx-phases (cubic MoC; PDF 89-2868 and orthorhombic Mo_2C; PDF 79-0744) suggest successful carburization of MoO_2 and a well-dispersed MoCx phase. This fact is consistent with the elemental analysis already described. The addition of a high amount of phosphorus slightly decreased the samples' crystallinity, increased the dispersion of MoCx-phase,[33] and produced nonsignificant XRD signals related to hexagonal and tetragonal-mixed phosphides phases (2θ = around 43.0; PDF 24-0771, PDF 89-5111).

NH_3-TPD characterizes the acid sites on the catalyst samples. In this way, the acid sites' strength is related to the NH_3-desorption temperature and the number of acid sites to the NH_3-desorbed quantity. For phosphorus-doped catalysts, the evaluation of acid sites is crucial for a better understanding of the changes in catalyst activity.[40,41] Analogous to conventional sulfided catalysts, phosphorus addition influences the catalyst acidity.[37] Table 2 shows the amount of NH_3 desorbed (mmol g^{-1}) and the corresponding temperature at maximums obtained during NH_3-TPD analyses.

Table 2. Amounts of NH_3 Desorbed and Temperature at Maximum Obtained during NH_3-TPD Analysis

catalyst	parameter	peak number			total
MoCx	peak number	1	2	3	
	temperature at maximum (°C)	177	253		
	quantity, NH_3 mmol g^{-1}	0.255	0.101		0.356
PMoCx 0.5	temperature at maximum (°C)	160	232	346	
	quantity, NH_3 mmol g^{-1}	0.173	0.256	0.108	0.537
PMoCx 1.5	temperature at maximum (°C)	175	260	367	
	quantity, NH_3 mmol g^{-1}	0.312	0.171	0.057	0.539
PMoCx 2.5	temperature at maximum (°C)	170	245		
	quantity, NH_3 mmol g^{-1}	0.261	0.364		0.625
PMoCx 3.5	temperature at maximum (°C)	171	242		
	quantity, NH_3 mmol g^{-1}	0.259	0.443		0.702
PMoCx 4.5	temperature at maximum (°C)	171	243		
	quantity, NH_3 mmol g^{-1}	0.301	0.391		0.692

The NH_3-TPD results show that phosphorus addition increased the number of weak (≤200 °C) and moderate acid sites (200−350 °C) of MoCx, with a maximum occurring at 3.5−4.5 wt % added phosphorus. Moreover, a phosphorus addition of up to 1.5 wt % also enhanced the acid centers' strength, increasing the number of strong acid sites (≥350 °C). Based on the previous research,[42] the acidity increase could be due to P−OH groups' formation on the catalyst surface. These changes in acid sites' amount and strength may be responsible for enhancing the hydrotreating activity,[33,40−44] which is analyzed later in the manuscript.

H_2-TPR analysis allows the evaluation of the effect of phosphorus addition on MoCx reducibility. As in the case of catalyst acidity, the study of the catalyst reduction is essential to understand the changes in hydrotreating activity due to phosphorus addition. Table 3 shows the H_2 consumption (mmol g^{-1}) and the corresponding temperature at maximums obtained during H_2-TPR.

The phosphorus addition affects the reducibility of MoCx, but the effect depends on its concentration. A phosphorus addition up to 1.5 wt % promoted the catalyst's reduction, which meant higher H_2 consumption at lower temperatures (range of 305−360 °C). This fact might be related to a higher site density, and consequently, improved catalysts' activity.[45] The trend changed at the higher phosphorus concentration, observing lower H_2 consumption for that range of temperatures and consequently lowers catalyst reduction. Thus, according to H_2-TPR results, PMoCx 0.5 and 1.5 catalysts are expected to be the most active due to higher reducibility over the range of temperatures used during processing. The absence of peaks at 584 °C demonstrates good carburization of the catalyst samples[39] as established by XRD (Figure 2) and elemental analysis (Table 1).

2.2. Catalyst Activity. The addition of phosphorus significantly influences the properties of the catalysts, such as acidity and reducibility. Therefore, phosphorus addition should also affect catalyst activity. This expectation is evaluated in the following section, considering the reaction products, their properties, and the crucial parameters of HDS and HDN effectiveness during AGO hydrotreating and AGO/RSO co-processing.

2.2.1. Reaction Products and Catalyst Selectivity. Analogous to previous experiments with carbide and nitride catalysts,[24] the first part of this study involves determining mass balance for each set of experimental conditions. Table S1 in the Supporting Information shows the mass balance results. "Mass closure", defined as the ratio between total outputs and total inputs multiplied by 100, was above 97.0% in all cases with an average of 97.4 ± 0.60%. This fact confirms suitable mass balance and reproducibility. As with MoCx,[24] an increase in the reaction temperature or a decrease in the WHSV leads to an increase in catalyst hydrocracking/hydrogenation activity, reflected in the higher production of gases. Sulfur- and nitrogen-containing species are the main compounds removed from the gas oil during hydrotreating. Triglycerides are converted into linear paraffins during co-processing with the concomitant formation of C_3H_8, CO_2, CO, and H_2O byproducts. This fact gives places a decrease in the yield of heavier organics favoring gaseous compounds and water production. This behavior was similar for all the tested catalysts.

Paraffins formed during co-processing were evaluated by Simdis. These compounds also were identified in detail and quantified by GC/MS−GC analysis at the higher RSO content (AGO/RSO = 75/25 wt %). Figure 3 shows the distribution of organic products generated by Simdis upon AGO processing under different operating conditions and upon co-processing with 95/5, 90/10, and 75/25 wt % AGO/RSO ratios over 0.5 and 4.5 wt % phosphorus-containing catalysts. Figure S1 in the Supporting Information shows the remaining Simdis analyses.

The Simdis results show the organic phase to be composed mainly of linear paraffins. No significant differences in the composition of hydrotreated gas oil due to operating conditions (temperature or WHSV) or phosphorus content in the catalysts were detected during AGO processing.

The linear paraffins content increases during co-processing due to triglyceride DO. This change, which occurs mainly in

https://dx.doi.org/10.1021/acsomega.0c06336
ACS Omega 2021, 6, 7680−7692

Table 3. H_2 Consumption and Temperature at Maximums of MoCx and PMoCx Catalysts after Passivation

catalyst	parameter	peak number				total
MoCx	peak number	1	2	3	4	
	temperature at maximum (°C)	381	398	433		
	consumption H_2 mmol g^{-1}	0.237	0.272	0.099		0.608
PMoCx 0.5						
	temperature at maximum (°C)	119	357	386	531	
	consumption H_2 mmol g^{-1}	0.021	0.319	0.223	0.075	0.638
PMoCx 1.5						
	temperature at maximum (°C)	305	340	467	513	
	consumption H_2 mmol g^{-1}	0.126	0.352	0.149	0.024	0.651
PMoCx 2.5						
	temperature at maximum (°C)	363	379	505	543	
	consumption H_2 mmol g^{-1}	0.260	0.083	0.239	0.017	0.599
PMoCx 3.5						
	temperature at maximum (°C)	335	446	528		
	consumption H_2 mmol g^{-1}	0.293	0.178	0.132		0.603
PMoCx 4.5						
	temperature at maximum (°C)	343	472	526		
	consumption H_2 mmol g^{-1}	0.286	0.213	0.106		0.605

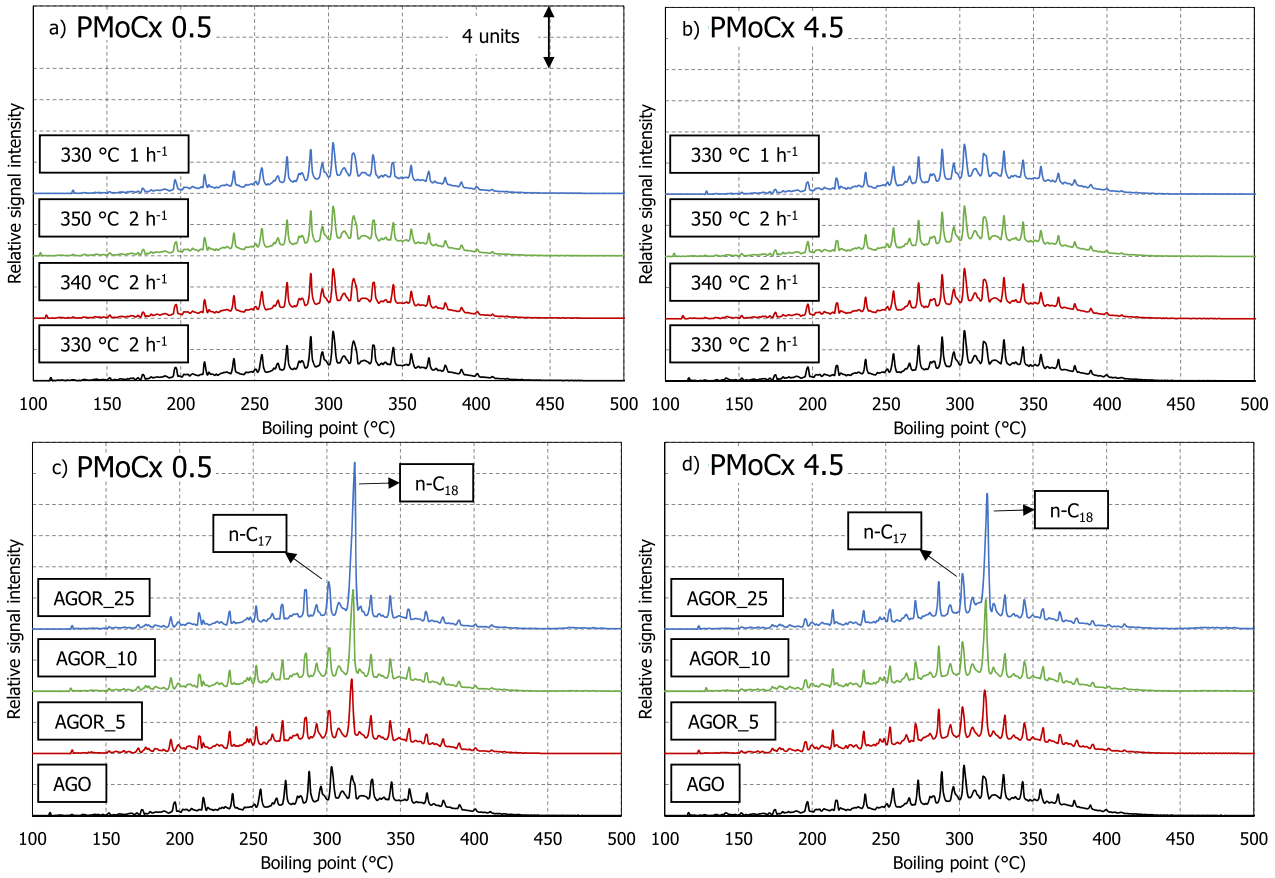

Figure 3. Simdis results of the organic phase produced upon AGO processing at operating conditions of 5.5 MPa, 330, 340, and 350 °C, and 1−2 h^{-1} (a, b) and AGO/RSO co-processing at 330 °C, 5.5 MPa and 2 h^{-1} with AGO/RSO ratios of 95/5, 90/10, and 75/25 wt % (c, d). The rest of the results are available in the Supporting Information.

the n-C_{15} to n-C_{18} paraffin range, increases the diesel fraction of the hydrotreated gas oil. A larger signal was detected for octadecane (317 °C) than for heptadecane (302 °C), which denotes a catalyst preference for the HDO pathway during triglyceride DO. This behavior is similar to that of the MoCx catalyst.[24] No waxes or white particles were detected among the organic products during co-processing, which indicates the complete conversion of triglycerides to paraffins.

A detailed analysis of the paraffin content in hydrotreated gas oil by GC/MS−GC is needed to evaluate the role of phosphorus addition in product distribution during co-processing. Table 4 shows the n-paraffin and isoparaffin content of the organic phase produced by AGO/RSO 75/25

https://dx.doi.org/10.1021/acsomega.0c06336
ACS Omega 2021, 6, 7680−7692

Table 4. N-Paraffin and Isoparaffin Content of the Organic Phase Obtained by AGO/RSO 75/25 Co-Processing Using PMoCx 0.5 and 4.5 Catalysts[a]

	PMoCx 0.5		PMoCx 4.5	
carbon atoms	n-paraffin, (w/w %)	isoparaffin, (w/w %)	n-paraffin, (w/w %)	isoparaffin, (w/w %)
9	0.06	0.07	0.05	0.08
10	0.21	0.28	0.25	0.26
11	0.56	0.70	0.60	0.68
12	0.72	0.90	0.78	0.88
13	0.83	1.41	0.94	1.34
14	1.04	1.27	1.01	1.51
15	1.44	1.17	1.41	1.37
16	2.72	1.76	2.40	1.89
17	3.02	2.72	3.52	2.65
18	13.49	2.65	10.52	3.62
19	1.43	3.28	1.40	2.08
20	1.77	2.95	1.47	2.74
21	0.97	1.60	0.85	1.37
22	0.98	1.24	0.72	1.15
23	0.57	0.89	0.41	0.87
24	0.44	0.61	0.29	0.58
25	0.23	0.40	0.16	0.38
26	0.17	0.28	0.17	0.25
27	0.02	0.20	0.03	0.17
total C_{15}–C_{18}	20.67	8.30	17.85	9.53
% HDO	78.0		72.0	
% DCO	22.0		28.0	

[a]The rest of the results are available in the Supporting Information.

co-processing over two different PMoCx catalysts. The HDO and DCO selectivities were calculated according to eqs 1 and 2. The remaining analyses are included in Table S2 in the Supporting Information.

These results confirm the promotion of the HDO pathway observed in Simdis, but with a light enhancement of the DCO pathway at higher phosphorus contents (from 22 to 28%). Related to isomerization, catalysts with higher phosphorus content also produced higher isoparaffins content (from 8.30 to 9.53%). These findings suggest that the increase in catalyst acidity of MoCx might promote the hydrocracking and isomerization activity of the catalysts.[46,47]

At the end of each stage, the reactor's outlet gas was analyzed to determine its composition. This fact enabled us to evaluate the effects of operating conditions and RSO co-processing on gas composition and the possible effect of the phosphorus content. During AGO processing, the outlet gas is primarily H_2 (98–99%) plus light gases such as CH_4, C_2H_6, and C_3H_8. CH_4 was the principal gaseous hydrocarbon product (85–95%) followed by C_2H_6 (1–3%), C_3H_8 (1–3%), and *n*-butane (1–2%). In the same line as mass balance results, an increase in temperature or a decrease in WHSV increase the production of the C_2–C_4 gases. This behavior was similar for all the tested catalysts. Although H_2 consumption and CH_4 production could be determined from the mass balance data, contamination of the H_2 source by the traces of CH_4 makes it hard to achieve an accurate mass balance for these compounds.

The production of light gases is higher during RSO co-processing than during AGO processing. This point is particularly true in C_3H_8, C_3H_6, and CO_2, which are the main gaseous side products obtained from the DO reaction.

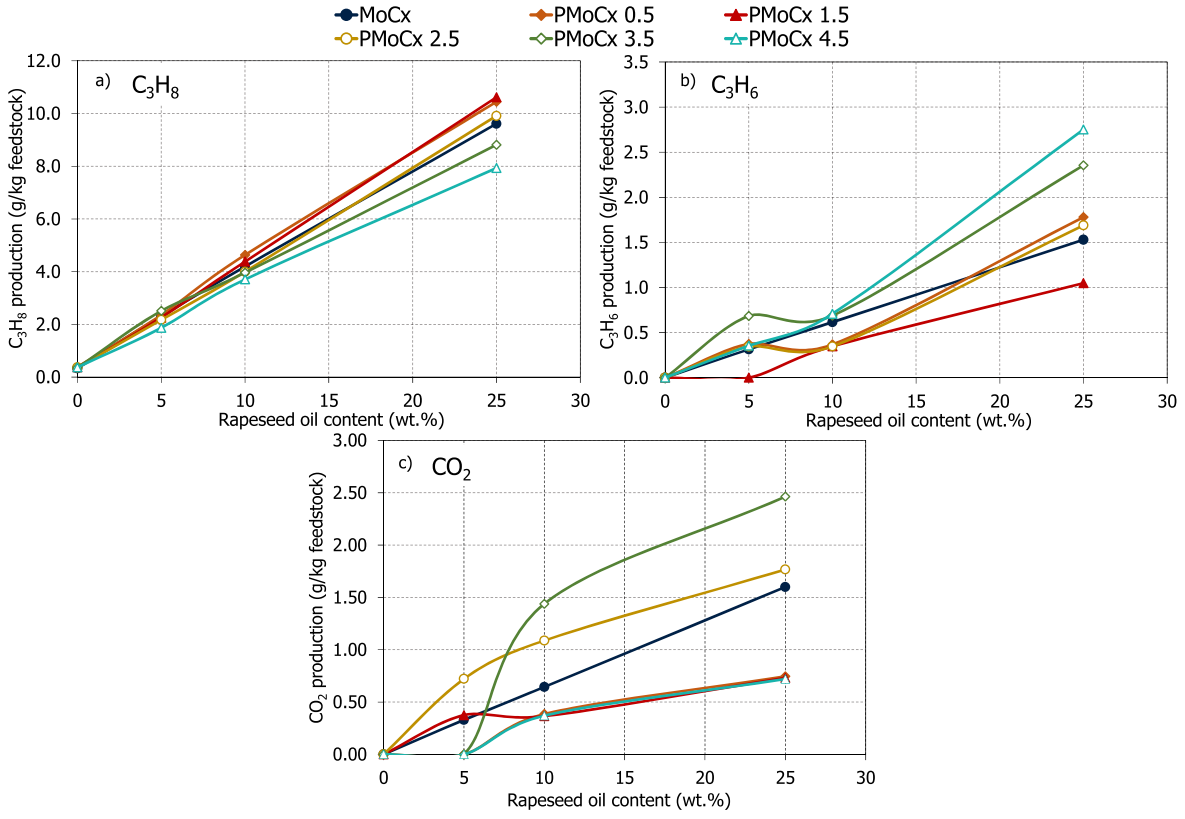

Figure 4. Propane (4a), propylene (4b), and carbon dioxide (4c) production per kg of feedstock during AGO/RSO co-processing at 330 °C, 5.5 MPa, 2 h^{-1} WHSV. Results at 0 wt % RSO correspond to 100 wt % AGO hydrotreating.

https://dx.doi.org/10.1021/acsomega.0c06336
ACS Omega 2021, 6, 7680–7692

Table 5. Basic Feedstocks Properties

property	AGO	RSO	AGO/RSO 95/5	AGO/RSO 90/10	AGO/RSO 75/25	standard test method
density at 20 °C (kg m^{-3})	851.3	914.5	854.6	857.5	867.0	ASTM D 4052
refractive index at 20 °C	1.4752	1.4756	1.4752	1.4752	1.4753	ASTM D 1218
S content (ppm)	11,200	2.3	10,600	10,100	8350	ASTM D 1552
N content (ppm)	239	22.9	210	195	170	ASTM D 5291
acid number (mg KOH g^{-1})	0.04	0.18				ASTM D 664
bromine index (mg Br g^{-1})	8211	41,929				ASTM D 1492
elemental analysis (%)						ISO 29541
C	86.0	75.6	85.5	85.0	83.4	
H	12.9	11.5	12.8	12.7	12.5	
O[a]	0.0	12.9	0.6	1.3	3.2	
Simdis (wt %)						ASTM D 2887
10	221	597				
30	280	606				
50	309	609				
70	336	612				
90	374	613				

[a]Oxygen content has been mathematically estimated, taking into account the C, H, S, and N contents.

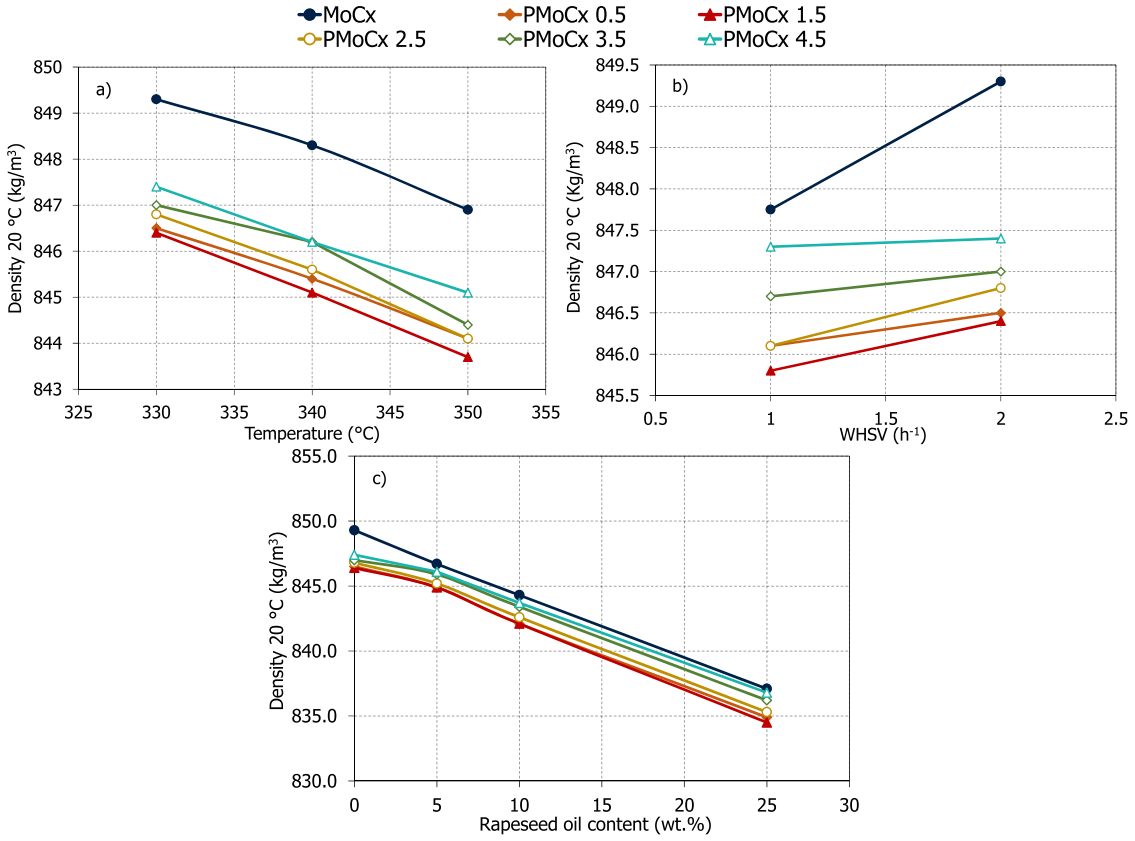

Figure 5. Organic phase densities measured at 20 °C for hydrotreating of 100 wt % AGO under different operating conditions (a, b) and during AGO/RSO co-processing (c).

Apart from H_2, the distributions were C_3H_8 (10−40%), C_3H_6 (2−10%), and CO_2 (0.5−5.5%). Figure 4 shows the C_3H_8, C_3H_6, and CO_2 production (g kg^{-1} of processed feedstock) as a function of the RSO content in the feedstock at 330 °C and 2 h^{-1}.

C_3H_8 production is a linear function of the RSO content (Figure 4a), consistent with the expectations of a triglyceride DO pathway.[10] However, changes in the phosphorus content of the catalyst produced interesting differences in C_3H_8 production. In this way, catalysts with up to 1.5 wt % phosphorus showed the highest C_3H_8 yields. To better understand this fact, it is necessary to study the C_3H_6 production (Figure 4b). C_3H_6 can be considered as a C_3H_8 precursor during the deoxygenation of triglycerides to n-paraffins.[48] Its presence is an indicator of lower hydrogenation activity because the catalyst cannot convert it to C_3H_8. Thus, catalysts that produce fewer C_3H_8 generate more C_3H_6, especially observable at higher RSO ratios in the feedstock. According to these results, it seems that a moderate increase in catalyst acidity in combination with higher catalyst reducibility

https://dx.doi.org/10.1021/acsomega.0c06336
ACS Omega 2021, 6, 7680−7692

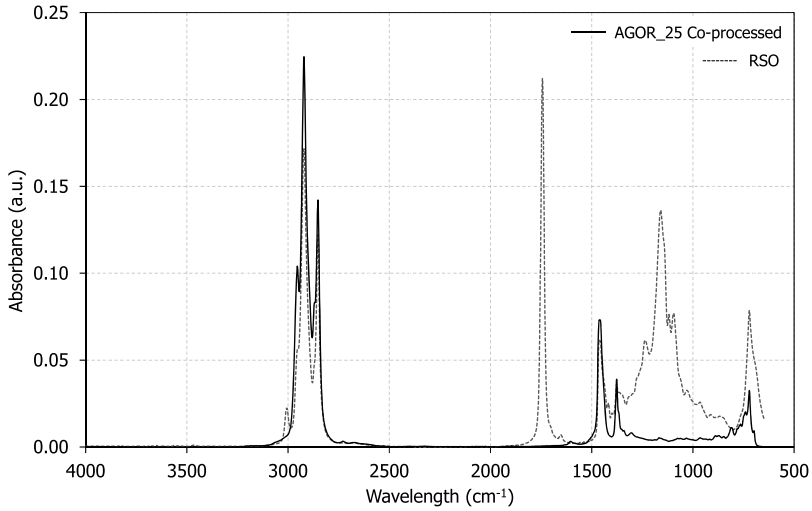

Figure 6. ATR-IR spectra of RSO feedstock and 75/25 wt % AGO/RSO products at 330 °C, 5.5 MPa, 2 h^{-1} WHSV.

positively affects the catalysts' hydrogenation activity, which in this case was observable as higher C_3H_8 yields.

It is not easy to make a detailed analysis of CO_2 production (Figure 4c) due to side reactions such as methanation or the reverse water−gas shift reaction in the presence of H_2. However, the enhanced production of CO_2 by the PMoCx 2.5 and 3.5 catalysts suggests a higher promotion of the DCO pathway by these catalysts, which is in line with the paraffin results determined by GC/MS−GC (Table 4).

2.2.2. Product Properties and Hydrotreating Effectiveness. This section evaluates the hydrotreated gas oil properties and the HDS and HDN catalyst efficiencies to study in-depth the effect of phosphorus addition on catalyst activity. The used feedstocks were from the same batches in all experiments. Table 5 shows their properties, consistent with expectations for a middle distillate and vegetable oil or a mixture of both of them.

Changes in temperature, WHSV, and RSO co-processing alter the density and other parameters of the products. Figure 5a−c shows the organic phase density obtained during AGO hydrotreating under different operating conditions and different AGO/RSO co-processing ratios. Higher reaction temperatures and lower WHSV's promoted the catalyst's hydrogenation/hydrocracking activity, which manifests as a decrease in product density. As in the case of propane production during co-processing, the moderate increase in catalyst acidity and higher reducibility due to phosphorus addition is responsible for promoting the hydrogenation activity of PMoCx catalysts. In this way, a phosphorus addition up to 1.5 wt % resulted in a lower product density. However, the trend reverses at >1.5 wt % phosphorus, and the product density increased.

Similar behavior was observed during co-processing. The catalysts with up to 1.5 wt % phosphorus showed lower densities than the others. In this case, the density decrease is not only related to triglyceride conversion,[49] which is assumed to be complete and identical for all catalyst samples, as it supports ATR-FTIR analysis[50] (Figure 6). This fact is due to a higher hydrogenation/hydrocracking activity of the AGO fraction, which results in better processing in terms of aromatic hydrogenation.

Other product properties, including elemental composition and acid number, remain unchanged. Table 6 shows the elemental analysis and acid number results of the liquid product obtained during PMoCx 0.5 testing at different operating conditions and AGO/RSO co-processing ratios. The remaining analyses are included in Table S3 in the Supporting Information.

Table 6. Elemental Analysis and Acid Numbers of Organic Phase Obtained during PMoCx 0.5 Catalyst Testing[a]

PMoCx 0.5	carbon content (%)	hydrogen content (%)	acid number (mg KOH g^{-1})
330 °C 5.5 MPa 2 h^{-1} AGO 100	86.6	13.3	0.02
340 °C 5.5 MPa 2 h^{-1} AGO 100	86.6	13.3	
350 °C 5.5 MPa 2 h^{-1} AGO 100	86.6	13.3	
330 °C 5.5 MPa 1 h^{-1} AGO 100	86.5	13.4	
330 °C 5.5 MPa 2 h^{-1} AGO/RSO 95/5	87.0	12.9	0.02
330 °C 5.5 MPa 2 h^{-1} AGO/RSO 90/10	87.0	12.9	0.02
330 °C 5.5 MPa 2 h^{-1} AGO/RSO 75/25	87.1	12.8	0.02

[a]The rest of the results are available in the Supporting Information.

However, the content of sulfur and nitrogen compounds of hydrotreated gas oil change significantly during the experiment depending on the operating conditions, co-processing ratio, or phosphorus amount in the catalyst. The HDS and HDN efficiencies were determined using eq 3, as described in the Materials and Methods. Figure 7 shows the HDS and HDN efficiencies during AGO processing and AGO/RSO co-processing at different catalyst phosphorus contents.

These results indicate there is a significant effect of phosphorus addition on HDS and HDN efficiencies. Like the effect observed in MoCx and MoNx catalysts already described by the authors,[24] the HDS/HDN efficiencies increased at higher temperatures and lower feed rates. This fact makes sense and is in line with the previous results described. Regarding the phosphorus content of catalysts, adding up to 1.5 wt % phosphorus significantly improved the HDS efficiency. This fact was especially noticeable for the PMoCx 1.5 catalyst, where it increased 5−10%, depending on

https://dx.doi.org/10.1021/acsomega.0c06336
ACS Omega 2021, 6, 7680−7692

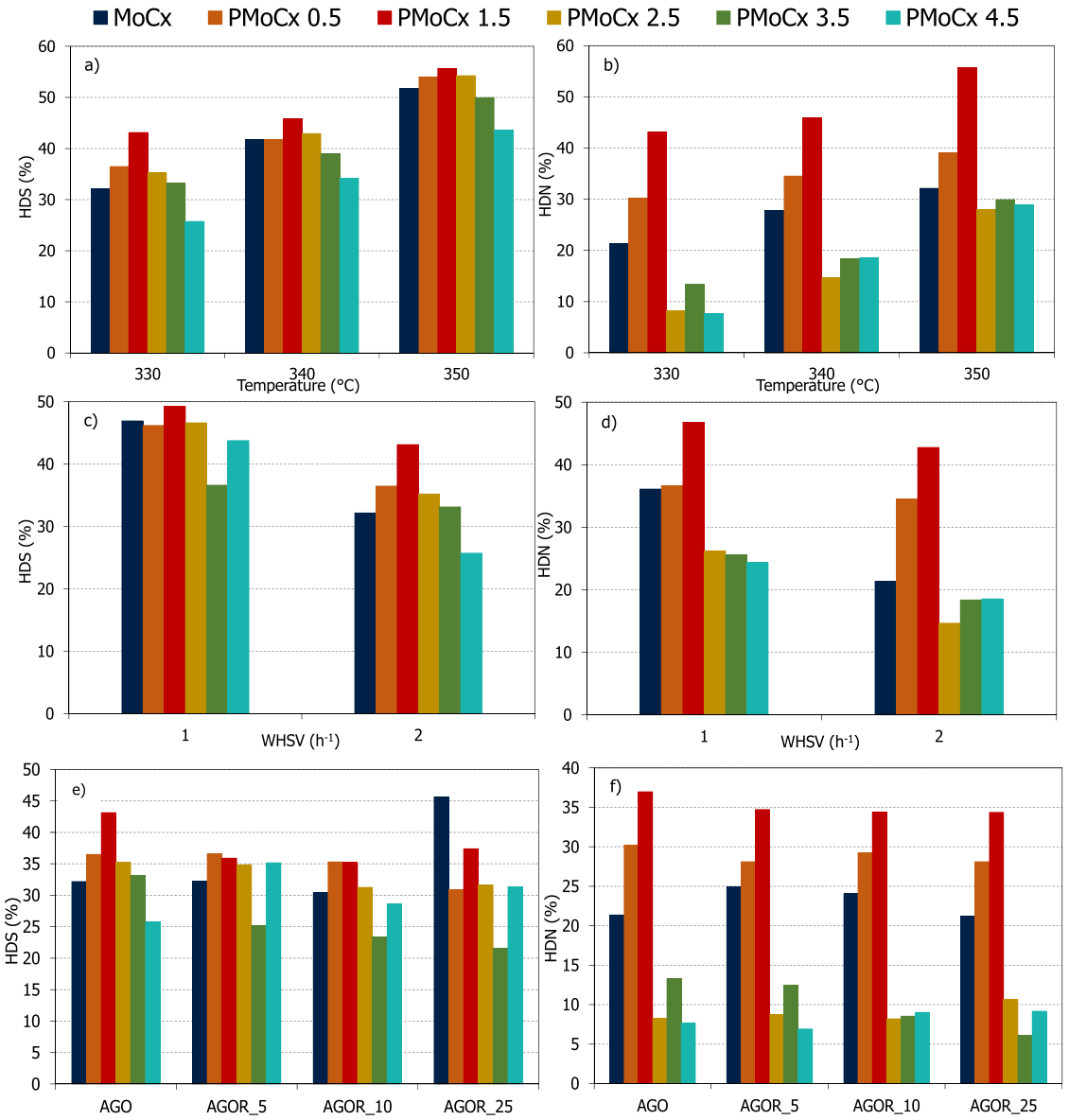

Figure 7. HDS and HDN efficiencies of MoCx and PMoCx catalysts under different operating conditions: 330−350 °C, 5.5 MPa, 1−2 h^{-1} (a−d) and during AGO/RSO co-processing at 330 °C, 5.5 MPa and 2 h^{-1} (e, f).

operating conditions. The synergic effect is even higher for HDN efficiencies,[33] where the increase was 10−25%. Analogous to previous results, there is a limit for the amount of phosphorus added, beyond which the HDS/HDN efficiencies begin to decrease. At this point, we conclude that the addition of up to 1.5 wt % of phosphorus produces a moderate increase in catalyst acidity and higher reducibility of the actives sites, resulting in a synergic effect on hydrotreating catalyst activity, mainly noticeable in HDS and HDN efficiencies.[41,51] However, higher amounts of phosphorus deteriorate the catalyst activity. According to the literature references, this effect could be due to phosphates compounds' formation on the catalytic surface.[52]

In RSO co-processing, the vegetable oil addition alters the catalyst activity pattern relative to that of AGO processing as a function of added phosphorus. RSO addition uniformly decreases HDS efficiency.[15] However, small amounts (0.5−1.5 wt %) of added phosphorus do increase HDS efficiency. The HDN efficiency behavior is similar to that observed during AGO processing. Thus, phosphorus addition up to 1.5 wt % increases HDN efficiency by 10−15%,[41] without a significant loss in HDN efficiency even at higher RSO ratios in the feedstock.

The highest HDS efficiency detected was lower than 60%, so catalyst stability was not evaluated in detail. However, during the catalyst testing, stages 1, 4, and 8 (Table 7) were at the same operating conditions, observing similar values for HDS/HDN efficiencies. This fact can be considered a fast indicative of catalyst stability for more than 200 h of processing. Figure 8 shows HDS and HDN efficiencies of PMoCx catalysts at 330 °C, 5.5 MPa, WHSV 2 h^{-1}.

3. CONCLUSIONS

Five sulfur-free Al_2O_3-supported and phosphorus-promoted MoCx catalysts (0.5, 1.5, 2.5, 3.5, and 4.5 wt %) were synthesized and tested for atmospheric gas oil hydrotreating and co-processing with rapeseed oil to study the catalyst properties and activity. The addition of phosphorus caused a

https://dx.doi.org/10.1021/acsomega.0c06336
ACS Omega 2021, 6, 7680−7692

Table 7. Description of Reaction Conditions (Chronological Order)

stage	TOS (time on stream) (h)	T (reactor temperature) (°C)	WHSV (h^{-1})	feed[a]	feed flow rate (g h^{-1})
1	0−40	330	2	AGO	16
2	40−64	340	2	AGO	16
3	64−88	350	2	AGO	16
4	88−112	330	2	AGO	16
5	112−136	330	2	AGOR_5	16
6	136−160	330	2	AGOR_10	16
7	160−184	330	2	AGOR_25	16
8	184−208	330	2	AGO	16
9	208−256	330	1	AGO	8

[a]AGOR_X: mixtures of AGO and RSO, X = wt % RSO.

loss of specific surface area and decreased mean pore diameter of the catalyst structure. However, these changes did not diminish catalyst activity due to an increase in catalyst acidity and reducibility. Phosphorus addition promotes the hydrocracking and isomeration reactions during co-processing, where hydrodeoxygenation was always the promoted pathway. Moreover, a moderate increase in catalyst acidity, the formation of strong acid sites, and higher active sites density resulted in lower organic phase density and decreasing sulfur and nitrogen content of hydrotreated gas oil. This behavior means improved hydrogenation activity, hydrodesulfurization (5−10%), and hydrodenitrogenation (10−25%) efficiencies during hydrotreating of atmospheric gas oil. Similar behavior occurred during co-processing, where the HDN efficiency shows the highest increase (10−15%) without a significant diminish upon the rapeseed oil addition. This fact mainly occurs for MoCx catalyst with phosphorus contents up to 1.5 wt %. Thus, our results allow us to point to the optimal phosphorus addition value, which significantly enhances MoCx/Al_2O_3 catalysts' hydrotreating activity. This work complements our previous studies and points to the next step for high activity sulfur-free catalysts development, with similar HDS/HDN efficiencies to the conventional hydrotreating catalysts.

4. MATERIALS AND METHODS

4.1. Feedstocks. Analogous to previous works,[24,30] the middle distillate used for co-processing was AGO, obtained from industrial atmospheric distillation of Russian export blend crude oil. The biomass component was food quality commercial RSO (supplied by ARO). The feedstocks and their mixtures (AGO/RSO = 95/5, 90/10, and 75/25 wt %) were characterized by following standard procedures: density at 20 °C (ASTM−American Society of Testing and Materials−D 4052), the refractive index at 20 °C (ASTM D 1218), sulfur (S: ASTM D 1552) and nitrogen (N: ASTM D 5291) content, acid number (ASTM D 664), elemental C, H analysis (ISO 29541), and simulated distillation (Simdis−ASTM D 2887). The triglycerides conversion into paraffin was verified by attenuated total reflection-Fourier transform infrared spectroscopy (ATR-FTIR). Standard refinery gas (97.5−99.5 vol % H_2 plus 0.5−2.5 vol % CH_4) was used as the H_2 supply.

4.2. Catalyst Synthesis and Characterization. Five sulfur-free Al_2O_3-supported (Sasol) phosphorus-modified MoCx catalysts (0.5, 1.5, 2.5, 3.5, and 4.5 wt % P) were prepared by the incipient wetness impregnation method. The synthesis of the MoCx catalyst has been described in previous articles.[24,38] A similar procedure was used to synthesize the phosphorus-promoted catalysts. This procedure is described briefly below.

A 48 g quantity of molybdate−hexamethylenetetramine complex was dissolved in a 70 mL aqueous 25% NH_3 solution at room temperature to prepare the impregnation solution. The Al_2O_3 support (60 g, 0.224−0.560 mm) was loaded with a molybdenum precursor and dried at 80 °C for 12 h. Subsequently, 16 g of the complex-impregnated precursor was further impregnated with an aqueous solution of diammonium phosphate to achieve phosphorus contents of 0.5, 1.5, 2.5, 3.5, and 4.5 wt %. The calculated portion of phosphate was dissolved in demineralized water to a total volume of 16 mL. The resulting intermediate was dried in an oven at 80 °C for 8 h with occasional stirring. The carburization of the active phase was achieved by a temperature-programmed reduction in a 100 cm long tubular quartz reactor having a 27 mm internal diameter (ID). The reactor was placed inside in a triple-zoned electric heater equipped with proportional-integral-derivative (PID) regulators. After impregnation, the support was treated by temperature-programmed reduction with a flow of 20 vol % CH_4 in H_2 starting from 200 to 700 °C (10 °C min^{-1}). The materials were held at the final temperature for 3 h. The reactor was cooled to ambient temperature and flushed with N_2. Finally,

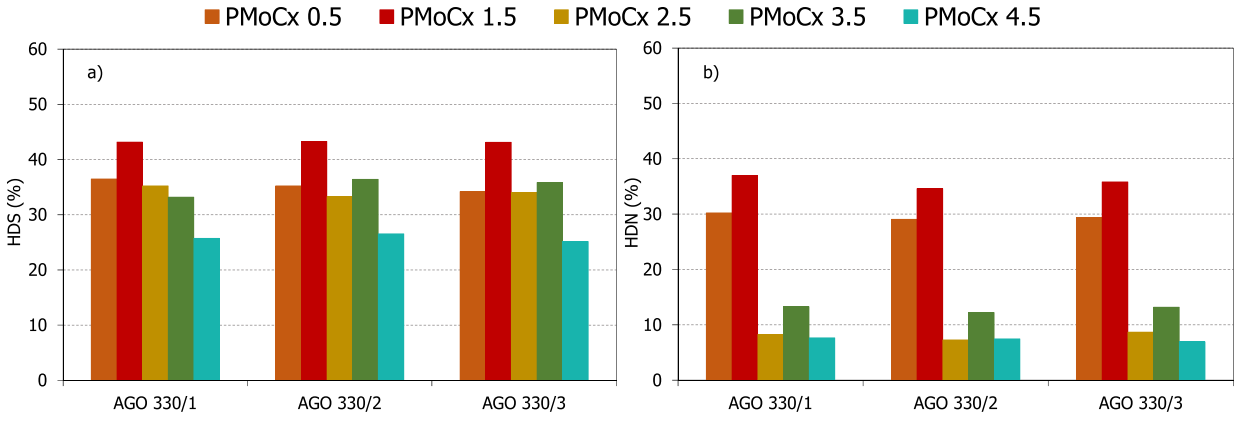

Figure 8. HDS (a) and HDN (b) efficiencies of MoCx and PMoCx catalysts under the same operating conditions (330, 5.5 MPa, 1−2 h^{-1}) but different times on stream (AGO 330/1−40 h; AGO 330/2−112 h; AGO 330/3−208 h).

https://dx.doi.org/10.1021/acsomega.0c06336
ACS Omega 2021, 6, 7680−7692

the catalysts were passivated under a flow of 1 vol % O_2 in Ar for 10 h. The catalysts were sieved immediately after synthesis to obtain a 0.224−0.560 mm fraction and loaded into the reactor.

Detailed characterization of the catalysts was performed after passivation. X-ray diffraction (XRD; Philips APD 1700) was used to identify the composition of the phases. Inductively coupled plasma spectroscopy (ICP; Agilent 725) and elemental analysis (FLASH 2000 Combustion CHNS/O analyzer) was used for composition analysis. The textural properties were characterized by the mercury porosimetry using an AutoPore IV 9510 (Micromeritics Instrument Corporation, Norcross, GA, USA) and by the nitrogen physisorption using an Autosorb iQ (Quantachrome Instruments, Boynton Beach, FL, USA). The specific surface area was calculated from the adsorption isotherm's linear plot using the Brunauer, Emmett and Teller (BET) Method in the pressure range of 0.05-0.30 P/P_0. Acidity and reducibility were measured by temperature-programmed desorption (NH_3-TPD) and temperature-programmed reduction (H_2-TPR), respectively, using an Autochem 2950 HP device (Micromeritics Instrument Corporation, Norcross, GA, USA).

4.3. Experimental Setup and Catalytic Tests. The hydrotreating and co-processing experiments were performed in the same unit used by the authors in previous experiments with carbide/nitride catalysts.[24,30] This unit consists of a bench-scale, 17 mm ID and 1.08 m length stainless steel reactor. Five thermocouples located in a 5 mm outer diameter (OD) thermowell were used to measure and control the internal temperature. The reactor was heated to the operating temperature using a triple-zone electric heater. Outlet lines were heated at 50 °C during co-processing to avoid plugging by unconverted products derived from biomass hydrotreating. The unit is in the experimental facility of ORLEN UniCRE (ORLEN Unipetrol Centre for Research and Education−Litvínov-Záluží, Czech Republic). Figure 9 shows a schematic diagram of the unit.

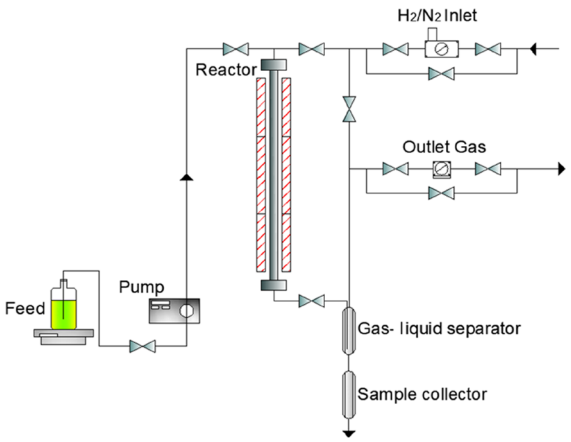

Figure 9. Schematic diagram of the experimental unit used for hydrotreating experiments (ORLEN UniCRE).

Analogous to previous experiments,[24,30] the catalyst bed consisted of 8.0 g of 0.224−0.560 mm PMoCx catalyst particles was divided into four parts (2.0 g each) and diluted with fine carborundum (SiC, 0.1 mm) in ratios of 1:1, 1:2, 1:3, and 1:4 (vol:vol). WHSV was calculated based on the catalyst bed's weight, which equates to a feedstock flow rate of 16 and 8 g h^{-1} for WHSV = 2 and 1 h^{-1}, respectively. The catalyst was loaded into the reactor from 1:1 (bottom) to 1:4 (top). This fact gradually increased the catalyst concentration along the reactor and maintained the isothermal regime's reaction temperature profile. After catalyst loading, the reactor was flushed with N_2 (flow rate = 600 NL h^{-1}) at 100 kPa and 25 °C for 2 h. Then, catalytic reduction started, the gas was changed to H_2 (50 NL h^{-1}), and the reactor was pressurized to 5.5 MPa and heated to 450 °C at 20 °C h^{-1}. After 4 h at these conditions, the temperature was reduced to 330 °C, the AGO feed was started (16 g h^{-1}), and the H_2 flow rate was adjusted to correspond to g L^{-1} = 1 NL g^{-1} h^{-1}.

The PMoCx catalysts were tested under the same conditions used previously[24,30] to compare with carbide and nitride catalysts. Table 7 summarizes the operating conditions used in the screening test. Stages 1, 4, and 8 are identical, which provides a short-term evaluation of catalyst stability.

Liquid products, which consisted primarily of hydrotreated gas oil and water (during co-processing only), were sampled and weighed every 4 h for mass balancing. Density at 20 °C (ASTM D 4052) and refractive index (ASTM D 1218) at 20 °C were determined for all samples taken. Steady state was achieved when these two parameters remained constant with time. The hydrotreated gas oil obtained at the steady state of each stage was characterized using the same analytical techniques employed for the feedstocks. The paraffin content (n- and iso-paraffins) during co-processing was determined by combined gas chromatography (GC) and mass spectrometry (MS) on 15 mg mL^{-1} sample dissolved in dichloromethane (GC/MS−GC system: Trace Ultra−Thermo Scientific; MS system: DSQ II−Thermo Scientific). Gas products were collected in a Tedlar bag at the end of each stage and analyzed off-line using an Agilent 7890A GC and Agilent's refinery gas analysis method. The instrument has three channels: (i) a HayeSep Q column with a thermal conductivity detector (TCD) to measure H_2 (N_2 carrier gas), (ii) a HayeSep Q column with a TCD to measure O_2, N_2, CO, CO_2, SH_2, and C_1−C_2 hydrocarbons (He carrier gas), and (iii) a 5A molecular sieve column with a flame ionization detector to measure C_1−C_7 hydrocarbons (He carrier gas).

4.4. Catalyst Selectivity and Hydrotreating Effectiveness. The catalyst's selectivity is determined by paraffin analysis of the proportion of even- and odd-numbered carbon atoms in the product chain. Equations 1 and 2 are explained in detail in the previous works:[4,24]

$$\text{HDO}\ [\%] = \frac{\sum(\text{even paraffin})}{\sum(\text{total paraffin [even + odd]})} \cdot 100, \quad (1)$$

$$\text{DCO}\ [\%] = \frac{\sum(\text{odd paraffin})}{\sum(\text{total paraffin [even + odd]})} \cdot 100, \quad (2)$$

"∑(even paraffin)" and "∑(odd paraffin)" represent the paraffin (wt %) produced by triglyceride hydrotreating via HDO (mainly n-C_{16} and n-C_{18}) and DCO (mainly n-C_{15} and n-C_{17}) pathways, respectively, and "∑(total paraffin [even + odd])" represents the total paraffin (wt %) formed solely by the hydrotreating of RSO. Hydrocarbon chain lengths typically occur in the n-C_{15} to the n-C_{18} range. The estimation assumes that no significant interaction occurs between AGO and RSO during co-processing.

https://dx.doi.org/10.1021/acsomega.0c06336
ACS Omega 2021, 6, 7680−7692

The hydrotreating effectiveness of sulfur and nitrogen removal (HDS and HDN, respectively) is defined as in previous manuscripts by eq 3:

$$\mathrm{HDX}\ (\%) = \frac{(X_0 - (X_p \cdot \eta))}{X_0} \cdot 100 \quad (3)$$

X = S, HDS/X = N, HDN

"X_0" and "X_p" represent the corresponding heteroatom contents of the feedstock (AGO, RSO, or the corresponding mixtures) and liquid product, respectively (wt ppm), and "η" is the quotient of the quantity of hydrotreating gas oil produced divided by that of the feedstock processed.

■ ASSOCIATED CONTENT

Supporting Information

The Supporting Information is available free of charge at https://pubs.acs.org/doi/10.1021/acsomega.0c06336.

Mass balances data and paraffins content, elemental analysis, acid number and Simdis of hydrotreated gas oil (PDF)

■ AUTHOR INFORMATION

Corresponding Author

Héctor de Paz Carmona − *ORLEN Unipetrol Centre for Research and Education (ORLEN UniCRE), Litvínov-Záluží 43670, Czech Republic;* orcid.org/0000-0002-8849-0977; Phone: +420-471-122-238; Email: hector.carmona@unicre.cz

Authors

Eliška Svobodová − *ORLEN Unipetrol Centre for Research and Education (ORLEN UniCRE), Litvínov-Záluží 43670, Czech Republic*

Zdeněk Tišler − *ORLEN Unipetrol Centre for Research and Education (ORLEN UniCRE), Litvínov-Záluží 43670, Czech Republic*

Uliana Akhmetzyanova − *ORLEN Unipetrol Centre for Research and Education (ORLEN UniCRE), Litvínov-Záluží 43670, Czech Republic*

Kateřina Strejcová − *ORLEN Unipetrol Centre for Research and Education (ORLEN UniCRE), Litvínov-Záluží 43670, Czech Republic*

Complete contact information is available at: https://pubs.acs.org/10.1021/acsomega.0c06336

Notes

The authors declare no competing financial interest.

■ ACKNOWLEDGMENTS

The work is a result of the project Development of the UniCRE Centre (LO1606), which has been financially supported by the Ministry of Education, Youth and Sports of the Czech Republic (MEYS) under the National Sustainability Programme I. The result was achieved using the infrastructure of the project Efficient Use of Energy Resources Using Catalytic Processes (LM2018119), which has been financially supported by MEYS within the targeted support of large infrastructures.

■ NOMENCLATURE

AGO	atmospheric gas oil
AGOR_X	mixtures of AGO and RSO, X = content of RSO
AGO/RSO	atmospheric gas oil and rapeseed oil mixtures
ASTM	American Society for Testing and Materials
ATR-FTIR	attenuated total reflection-Fourier transform infrared spectroscopy
BET	Brunauer−Emmett−Teller method
CFPP	cold filter plugging point
DO	deoxygenation
EU	European Union
GC	gas chromatography
DCO	(hydro)decarboxylation and (hydro)-decarbonylation
HDN	hydrodenitrogenation
HDO	hydrodeoxygenation
HDS	hydrodesulfurization
ICP-OES	inductively coupled plasma optical emission spectroscopy
ID	internal diameter (mm)
MoCx	molybdenum carbide catalysts
MoNx	molybdenum nitride catalysts
MS	mass spectrometry
N	nitrogen content
OD	outer diameter (mm)
PDF	powder diffraction files
PID	proportional-integral-derivative
PMoCx	phosphorus promoted molybdenum carbide catalysts
RED	renewable energy directive
RSO	rapeseed oil
S	sulfur content
S_{BET}	BET surface areas (m^2/g)
Simdis	simulated distillation
TCD	thermal conductivity detector
TOS	time on stream (h)
TPD	temperature-programmed desorption
TPR	temperature-programmed reduction
UniCRE	Unipetrol Centre for Research and Education
WHSV	weight hourly space velocity (h^{-1})

■ REFERENCES

(1) Bezergianni, S.; Dimitriadis, A.; Kikhtyanin, O.; Kubička, D. Refinery co-processing of renewable feeds. *Prog. Energy Combust. Sci.* **2018**, *68*, 29−64.

(2) Al-Sabawi, M.; Chen, J. Hydroprocessing of Biomass-Derived Oils and Their Blends with Petroleum Feedstocks: A Review. *Energy Fuels* **2012**, *26*, 5373−5399.

(3) Liu, Y.; Sotelo-Boyás, R.; Murata, K.; Minowa, T.; Sakanishi, K. Hydrotreatment of Vegetable Oils to Produce Bio-Hydrogenated Diesel and Liquefied Petroleum Gas Fuel over Catalysts Containing Sulfided Ni-Mo and Solid Acids. *Energy Fuels* **2011**, *25*, 4675−4685.

(4) De Paz Carmona, H.; de la Torre Alfaro, O.; Brito Alayón, A.; Romero Vázquez, M. A.; Macías Hernández, J. J. Co-processing of straight run gas oil with used cooking oil and animal fats. *Fuel* **2019**, *254*, 115583.

(5) Mikkonen, S. Second-generation renewable diesel offers advantages : Hydrotreated vegetable oils are more compatible with engine design and operations : Clean Fuels. *Hydrocarbon process.* **2008**, *87*, 63−66.

(6) Arun, N.; Sharma, R. V.; Dalai, A. K. Green diesel synthesis by hydrodeoxygenation of bio-based feedstocks: strategies for catalyst design and development. *Renewable Sustainable Energy Rev.* **2015**, *48*, 240−255.

(7) Hollak, S. Catalytic Deoxygenation of Fatty Acids and Triglycerides for Production of Fuels and Chemicals. Ph.D. Thesis, Utrecht University, Utrecht, The Netherlands, 2014.

(8) Bezergianni, S.; Dimitriadis, A. Comparison between different types of renewable diesel. *Renewable Sustainable Energy Rev.* **2013**, *21*, 110−116.
(9) Gosselink, R. W.; Hollak, S. A. W.; Chang, S.-W.; van Haveren, J.; de Jong, K. P.; Bitter, J. H.; van Es, D. S. Reaction Pathways for the Deoxygenation of Vegetable Oils and Related Model Compounds. *ChemSusChem* **2013**, *6*, 1576−1594.
(10) Kubičková, I.; Kubička, D. Utilization of Triglycerides and Related Feedstocks for Production of Clean Hydrocarbon Fuels and Petrochemicals: A Review. *Waste Biomass Valorization* **2010**, *1*, 293−308.
(11) Díaz de León, J. N.; Ramesh Kumar, C.; Antúnez-García, J.; Fuentes-Moyado, S. Recent Insights in Transition Metal Sulfide Hydrodesulfurization Catalysts for the Production of Ultra Low Sulfur Diesel: A Short Review. *Catalysts* **2019**, *9*, 87.
(12) Tanimu, A.; Alhooshani, K. Advanced Hydrodesulfurization Catalysts: A Review of Design and Synthesis. *Energy Fuels* **2019**, *33*, 2810−2838.
(13) Bezergianni, S.; Dimitriadis, A.; Meletidis, G. Effectiveness of CoMo and NiMo catalysts on co-hydroprocessing of heavy atmospheric gas oil-waste cooking oil mixtures. *Fuel* **2014**, *125*, 129−136.
(14) Egeberg, R.; Michaelsen, N.; Skyum, L.; Zeuthen, P. Hydrotreating in the production of green diesel. *Digital Refin.* **2010**, 1−11.
(15) Kubička, D.; Horáček, J. Deactivation of HDS catalysts in deoxygenation of vegetable oils. *Appl. Catal., A* **2011**, *394*, 9−17.
(16) Kochetkova, D.; Blažek, J.; Šimáček, P.; Staš, M.; Beňo, Z. Influence of rapeseed oil hydrotreating on hydrogenation activity of CoMo catalyst. *Fuel Process. Technol.* **2016**, *142*, 319−325.
(17) Furimsky, E. Metal carbides and nitrides as potential catalysts for hydroprocessing. *Appl. Catal., A* **2003**, *240*, 1−28.
(18) Miles, C. E.; Carlson, T. R.; Morgan, B. J.; Topalian, P. J.; Schare, J. R.; Bussell, M. E. Hydrodesulfurization properties of Nickel Phosphide on Boron-treated Alumina supports. *ChemCatChem* **2020**, 4939.
(19) Golubeva, M. A.; Zakharyan, E. M.; Maximov, A. L. Transition Metal Phosphides (Ni, Co, Mo, W) for Hydrodeoxygenation of Biorefinery Products (a Review). *Pet. Chem.* **2020**, *60*, 1109−1128.
(20) Li, X.; Luo, X.; Jin, Y.; Li, J.; Zhang, H.; Zhang, A.; Xie, J. Heterogeneous sulfur-free hydrodeoxygenation catalysts for selectively upgrading the renewable bio-oils to second generation biofuels. *Renewable Sustainable Energy Rev.* **2018**, *82*, 3762−3797.
(21) Ramanathan, S.; Yu, C. C.; Oyama, S. T. New Catalysts for Hydroprocessing: Bimetallic Oxynitrides: II. Reactivity Studies. *J. Catal.* **1998**, *173*, 10−16.
(22) Phimsen, S.; Kiatkittipong, W.; Yamada, H.; Tagawa, T.; Kiatkittipong, K.; Laosiripojana, N.; Assabumrungrat, S. Nickel sulfide, nickel phosphide and nickel carbide catalysts for biohydrotreated fuel production. *Energy Convers. Manage.* **2017**, *151*, 324−333.
(23) Dhandapani, B.; Clair, T. S.; Oyama, S. T. Simultaneous hydrodesulfurization, hydrodeoxygenation, and hydrogenation with molybdenum carbide. *Appl. Catal., A* **1998**, *168*, 219−228.
(24) de Paz Carmona, H.; Horáček, J.; Tišler, Z.; Akhmetzyanova, U. Sulfur free supported MoCx and MoNx Catalysts for the hydrotreatment of Atmospheric gasoil and its blends with rapeseed oil. *Fuel* **2019**, *254*, 115582.
(25) Sousa, L. A.; Zotin, J. L.; Teixeira da Silva, V. Hydrotreatment of sunflower oil using supported molybdenum carbide. *Appl. Catal., A* **2012**, *449*, 105−111.
(26) Shamanaev, I. V.; Deliy, I. V.; Aleksandrov, P. V.; Reshetnikov, S. I.; Bukhtiyarova, G. A. Methyl palmitate hydrodeoxygenation over silica-supported nickel phosphide catalysts in flow reactor: experimental and kinetic study. *J. Chem. Technol. Biotechnol.* **2019**, 3007.
(27) Wang, F.; Xu, J.; Jiang, J.; Liu, P.; Li, F.; Ye, J.; Zhou, M. Hydrotreatment of vegetable oil for green diesel over activated carbon supported molybdenum carbide catalyst. *Fuel* **2018**, *216*, 738−746.
(28) Horáček, J.; Akhmetzyanova, U.; Skuhrovcová, L.; Tišler, Z.; de Paz Carmona, H. Alumina-supported MoNx, MoCx and MoPx catalysts for the hydrotreatment of rapeseed oil. *Appl. Catal., B* **2020**, *263*, 118328.
(29) Akhmetzyanova, U.; Tišler, Z.; Sharkov, N.; Skuhrovcová, L.; Pelíšková, L.; Kikhtyanin, O.; Mäki-Arvela, P.; Opanasenko, M.; Peurla, M.; Murzin, D. Y. Molybdenum Nitrides, Carbides and Phosphides as Highly Efficient Catalysts for the (hydro)-Deoxygenation Reaction. *ChemistrySelect* **2019**, *4*, 8453−8459.
(30) de Paz Carmona, H.; Akhmetzyanova, U.; Tišler, Z.; Vondrová, P. Hydrotreating atmospheric gasoil and co-processing with rapeseed oil using supported Ni-Mo and Co-Mo carbide catalysts. *Fuel* **2020**, *268*, 117363.
(31) Diaz, B.; Sawhill, S. J.; Bale, D. H.; Main, R.; Phillips, D. C.; Korlann, S.; Self, R.; Bussell, M. E. Hydrodesulfurization over supported monometallic, bimetallic and promoted carbide and nitride catalysts. *Catal. Today* **2003**, *86*, 191−209.
(32) Guangzhou, J.; Jianhua, Z.; Xiuju, F.; Guida, S.; Junbin, G. Effect of Ni promoter on Dibenzothiophene Hydrodesulfurization Performance of Molybdenum carbide catalyst. *Chinese J. Catal.* **2006**, *27*, 899−903.
(33) Sundaramurthy, V.; Dalai, A. K.; Adjaye, J. Effect of phosphorus addition on the hydrotreating activity of $NiMo/Al_2O_3$ carbide catalyst. *Catal. Today* **2007**, *125*, 239−247.
(34) Maity, S. K.; Ancheyta, J.; Rana, M. S.; Rayo, P. Effect of phosphorus on activity of hydrotreating catalyst of Maya heavy crude. *Catal. Today* **2005**, *109*, 42−48.
(35) Da Costa, P.; Potvin, C.; Manoli, J. M.; Breysse, M.; Djéga-Mariadassou, G. Novel phosphorus-doped alumina-supported molybdenum and tungsten carbides: synthesis, characterization and hydrogenation properties. *Catal. Lett.* **2001**, *72*, 91−97.
(36) Jian, M.; Kapteijn, F.; Prins, R. Kinetics of the hydrodenitrogenation of *ortho*-propylaniline over $NiMo(P)Al_2O_3$ Catalysts. *J. Catal.* **1997**, *168*, 491−500.
(37) Prada Silvy, R. Parameters controlling the scale-up of $CoMoP/\Upsilon\text{-}Al_2O_3$ and $NiMoP/\Upsilon\text{-}Al_2O_3$ catalysts for the hydrotreating and mild-hydrocracking of heavy gasoil. *Catal. Today* **2019**, *338*, 93−99.
(38) Tišler, Z.; Velvarská, R.; Skuhrovcová, L.; Pelíšková, L.; Akhmetzyanova, U. Key role of precursor nature in phase composition of supported molybdenum carbides and nitrides. *Materials* **2019**, *12*, 415.
(39) Sundaramurthy, V.; Dalai, A. K.; Adjaye, J. Comparison of P-containing $\gamma\text{-}Al_2O_3$ supported Ni-Mo bimetallic carbide, nitride and sulfide catalysts for HDN and HDS of gas oils derived from Athabasca bitumen. *Appl. Catal., A* **2006**, *311*, 155−163.
(40) Ferdous, D.; Dalai, A. K.; Adjaye, J. A series of $NiMo/Al_2O_3$ catalysts containing boron and phosphorus: Part I. Synthesis and characterization. *Appl. Catal., A* **2004**, *260*, 137−151.
(41) Ferdous, D.; Dalai, A. K.; Adjaye, J. A series of $NiMo/Al_2O_3$ catalysts containing boron and phosphorus: Part II. Hydrodenitrogenation and hydrodesulfurization using heavy gas oil derived from Athabasca bitumen. *Appl. Catal., A* **2004**, *260*, 153−162.
(42) Sundaramurthy, V.; Dalai, A. K.; Adjaye, J. The effect of phosphorus on hydrotreating property of $NiMo/\Upsilon\text{-}Al_2O_3$ nitride catalyst. *Appl. Catal., A* **2008**, *335*, 204−210.
(43) Lewandowski, M.; Sarbak, Z. The effect of boron addition on hydrodesulfurization and hydrodenitrogenation activity of $NiMo/Al_2O_3$ catalysts. *Fuel* **2000**, *79*, 487−495.
(44) Vatutina, Y. V.; Klimov, O. V.; Stolyarova, E. A.; Nadeina, K. A.; Danilova, I. G.; Chesalov, Y. A.; Gerasimov, E. Y.; Prosvirin, I. P.; Noskov, A. S. Influence of the phosphorus addition ways on properties of CoMo-catalysts of hydrotreating. *Catal. Today* **2019**, *329*, 13−23.
(45) Perez-Romo, P.; Potvin, C.; Manoli, J.-M.; Chehimi, M. M.; Djéga-Mariadassou, G. Phosphorus-Doped Molybdenum Oxynitrides and Oxygen-Modified Molybdenum Carbides: Synthesis, Characterization, and Determination of Turnover Rates for Propene Hydrogenation. *J. Catal.* **2002**, *208*, 187−196.

https://dx.doi.org/10.1021/acsomega.0c06336
ACS Omega 2021, 6, 7680−7692

(46) Artetxe, M.; Lopez, G.; Amutio, M.; Elordi, G.; Bilbao, J.; Olazar, M. Cracking of High Density Polyethylene Pyrolysis Waxes on HZSM-5 Catalysts of Different Acidity. *Ind. Eng. Chem. Res.* **2013**, *52*, 10637−10645.
(47) Cardó, X.; Bergadà, O.; Cesteros, Y.; Salagre, P. Effect of catalyst acidity and porosity on the catalytic isomerization of linoleic acid to obtain conjugated linoleic acids (CLAs). *Chem. Eng. J.* **2012**, *183*, 459−465.
(48) Mäki-Arvela, P.; Kubickova, I.; Snåre, M.; Eränen, K.; Murzin, D. Y. Catalytic Deoxygenation of Fatty Acids and Their Derivatives. *Energy Fuels* **2007**, *21*, 30−41.
(49) Walendziewski, J.; Stolarski, M.; Łużny, R.; Klimek, B. Hydroprocessing of light gas oil − rape oil mixtures. *Fuel Process. Technol.* **2009**, *90*, 686−691.
(50) Pinto, F.; Martins, S.; Gonçalves, M.; Costa, P.; Gulyurtlu, I.; Alves, A.; Mendes, B. Hydrogenation of rapeseed oil for production of liquid bio-chemicals. *Appl. Energy* **2013**, *102*, 272−282.
(51) Dhandapani, B.; Ramanathan, S.; Yu, C. C.; Frühberger, B.; Chen, J. G.; Oyama, S. T. Synthesis, Characterization, and Reactivity Studies of Supported Mo_2C with Phosphorus Additive. *J. Catal.* **1998**, *176*, 61−67.
(52) Santillán-Vallejo, L. A.; Melo-Banda, J. A.; Reyes de la Torre, A. I.; Sandoval-Robles, G.; Domínguez, J. M.; Montesinos-Castellanos, A.; de los Reyes-Heredia, J. A. Supported (NiMo, CoMo)-carbide, −nitride phases: Effect of atomic ratios and phosphorus concentration on the HDS of thiophene and dibenzothiophene. *Catal. Today* **2005**, *109*, 33−41.

https://dx.doi.org/10.1021/acsomega.0c06336
ACS Omega 2021, 6, 7680−7692